8. Sotozono C, Ueta M, Koizumi N, Inatomi T, Ikezawa Z, Shirakata Y, Hashimoto K, Kinoshita S. Diagnosis and Treatment of Stevens-Johnson Syndrome and Toxic Epidermal Necrolysis with Ocular Complications. Ophthalmology. 2009;116:685-690.

9. Araki Y, Sotozono C, Inatomi T, Ueta M, Yokoi N, Ueda E, Kishimoto S, Kinoshita S. Successful Treatment of Stevens-Johnson Syndrome with Steroid Pulse Therapy at Disease Onset. Am J Ophthalmol. 2009;147:1004-1011.

10. Yamada J, Hamuro J, Fukushima A, Ohteki T, Terai K, Iwakura Y, Yagita H, Kinoshita S. MHC-matched corneal allograft rejection in an IFN-gamma/IL-17-independent manner in C57BL/6 mice. Invest Ophthalmol Vis Sci. 2009;50:2139-2146.

11. Connon CJ, Doutch J, Chen B, Hopkinson A, Mehta JS, Nakamura T, Kinoshita S. Meek KM: The Variation In Transparency Of Amniotic Membrane Used In Ocular Surface Regeneration. Br J Ophthalmol. 2009;Mar 19:[Epub ahead of print].

12. Matsuda A, Okayama Y, Terai N, Yokoi N, Ebihara N, Tanioka H, Kawasaki S, Inatomi T, Katoh N, Ueda E, Hamuro J, Murakami A, Kinoshita S. The role of interleukin-33 in chronic allergic conjunctivitis. Characteristic morphology and distribution of bone marrow derived cells in the cornea. Invest Ophthalmol Vis Sci. 2009;50(10):4646-4652.

13. Koizumi H, Maruyama K, Kinoshita S. Blue light and near-infrared fundus autofluorescence in acute Vogt-Koyanagi-Harada disease. Br J Ophthalmol. 2009;Dec 3:[Epub ahead of print].

14. Ang L, Tanioka H, Kinoshita S . Cultivated Human Conjunctival Epithelial Transplantation For Total Limbal Stem Cell Deficiency. Invest Ophthalmol Vis Sci. 2009;Jul 30:[Epub ahead of print].

15. Tanioka H, Yokoi N, Komuro A, , Kawasaki S, Matsuda A, Kinoshita S. Investigation of the corneal filament in filamentary keratitis. Invest Ophthalmol Vis Sci. 2009;50(8):3696-3702.
16. Okumura N, Ueno M, Koizumi N, Sakamoto Y, Hirata K, Hamuro J, Kinoshita S. enhancement on primate corneal endothelial cell survival in vitro by a ROCK inhibitor. Invest Ophthalmol Vis Sci. 2009;50(8):3680-3687.
17. Ouchi M, Kinoshita S. Prospective Randomised trial of limbal relaxing incision combined with microincision cataract surgery. Refract Surg. 2009;Oct. 26:1-6: [Epub ahead of print].
18. Matsuda A, Ebihara N, Yokoi N, Kawasaki S, Tanioka H, Inatomi T, Malefyt R, Hamuro J, Kinoshita S, Murakami A. Functional Roles of Thymic Stromal Lymphopoietin for Chronic Allergic Keratoconjunctivitis. Invest Ophthalmol Vis Sci. 2009;Sep 9:[Epub ahead of print].
19. Matsuda A, Okayama Y, Ebihara N, Yokoi N, Hamuro J, Walls AF, Ra Chisei, Hopkin JM, Kinoshita S. Hyperexpression of the high affinity IgE receptor- β chain in chronic allergic keratoconjuctivitis. Invest Ophthalmol Vis Sci. 2009;50(6):2871-2877

研究分担者　森　和彦

1. Nakano M, Ikeda Y, Taniguchi T, Yagi T, Fuwa M, Omi N, Tokuda Y, Tanaka M, Yoshii K, Kageyama M, Naruse S, Matsuda A, Mori K, Kinoshita S, Tashiro K. Three susceptible loci associated with primary open-angle glaucoma identified by genome-wide association study in a Japanese population. Proc Natl Acad Sci U S A. 2009;4;106(31):12838-12842.
2. Nakano M, Ikeda Y, Yagi T, Mori K, Kinoshita S, Tashiro K. Reply to Rao

et al.: Appropriate study design for genome-wide association study replication to identify variants modestly associated with complex traits. Proc Natl Acad Sci U.S.A. 2009;106(44):125-126.

3. 森　和彦. 森式直立型手術用ゴニオレンズ(森ゴニオレンズ)　眼科手術(0914-6806)22巻3号 Page349-351(2009.07)
4. 森　和彦. 【続発緑内障は変わった!】 角膜移植後の緑内障はこう治す(解説/特集)　あたらしい眼科(0910-1810)26巻3号 Page317-321(2009.03)

研究分担者　田代　啓

1. Nakano M, Ikeda Y, Taniguchi T, Yagi T, Fuwa M, Omi N, Tokuda Y, Tanaka M, Yoshii K, Kageyama M, Naruse S, Matsuda A, Mori K, Kinoshita S, Tashiro K. Three susceptible loci associated with primary open-angle glaucoma identified by genome-wide association study in a Japanese population. Proc. Natl. Acad. Sci. U.S.A. 2009;106(31): 12838-12842.
2. Nakano M, Ikeda Y, Yagi T, Mori K, Kinoshita S, Tashiro K. Reply to Rao et al.: Appropriate study design for genome-wide association study replication to identify variants modestly associated with complex traits. Proc. Natl. Acad. Sci. U.S.A. 2009;106(44):125-126.

研究分担者　長崎　生光

1. Nagasaki I, Kawakami T, Hara Y, Ushitaki, F: The Borsuk-Ulam theorem in a real closed field, Far East J. Math. Sci. (FJMS). 2009;33:113-124.
2. Nagasaki I: A note on the existence problem of isovariant maps between

representation spaces, Studia Humana et Naturalia. 2009;43:33-42.

［Ⅳ］

研究成果の刊行物・別刷

Three susceptible loci associated with primary open-angle glaucoma identified by genome-wide association study in a Japanese population

Masakazu Nakano[a,1], Yoko Ikeda[b,1], Takazumi Taniguchi[a,c,1], Tomohito Yagi[a], Masahiro Fuwa[a,c], Natsue Omi[a], Yuichi Tokuda[a], Masami Tanaka[a], Kengo Yoshii[a], Masaaki Kageyama[c], Shigeta Naruse[b], Akira Matsuda[b], Kazuhiko Mori[b], Shigeru Kinoshita[b,2], and Kei Tashiro[a,2]

Departments of [a]Genomic Medical Sciences and [b]Ophthalmology, Kyoto Prefectural University of Medicine, Kawaramachi-Hirokoji, Kamigyo-ku, Kyoto 602-8566, Japan; and [c]Research and Development Center, Santen Pharmaceutical Co., Ltd., 8916-16 Takayama-cho, Ikoma, Nara 630-0101, Japan

Communicated by Tasuku Honjo, Kyoto University, Kyoto, Japan, June 10, 2009 (received for review March 28, 2009)

Primary open-angle glaucoma (POAG) is the major type of glaucoma. To discover genetic markers associated with POAG, we examined a total of 1,575 Japanese subjects in a genome-wide association study (stage 1) and a subsequent study (stage 2). Both studies were carried out at a single institution. In the stage 1 association study, we compared SNPs between 418 POAG patients and 300 control subjects. First, low-quality data were eliminated by a stringent filter, and 331,838 autosomal SNPs were selected for analysis. Poorly clustered SNPs were eliminated by a visual assessment, leaving 255 that showed a significant deviation ($P < 0.001$) in the allele frequency comparison. In the stage 2 analysis, we tested these 255 SNPs for association in DNA samples from a separate group of 409 POAG and 448 control subjects. High-quality genotype data were selected and used to calculate the combined P values of stages 1 and 2 by the Mantel–Haenszel test. These analyses yielded 6 SNPs with $P < 0.0001$. All 6 SNPs showed a significant association ($P < 0.05$) in stage 2, demonstrating a confirmed association with POAG. Although we could not link the SNPs to the annotated gene(s), it turned out that we have identified 3 genetic loci probably associated with POAG. These findings would provide the foundation for future studies to build on, such as for the metaanalysis, to reveal the molecular mechanism of the POAG pathogenesis.

diagnosis | SNP | GWAS | meta-analysis | glaucoma genetics

Glaucoma is a neurodegenerative disease of the eye, and it is one of the leading causes of blindness worldwide (1). It is characterized by a specific pattern of optic nerve degeneration and visual field defects. The diagnosis of glaucoma preceding the development of visual field defects is commonly made by observing optic nerve degeneration, which manifests, on fundus examination, as an enlarged optic disc cup and a damaged retinal nerve-fiber layer. Because early drug treatment, just after the onset of visual field damage, is quite effective in slowing the irreversible progression of glaucoma (2–4), routine fundus examinations of the optic nerve and visual field tests are desirable. However, because of the restriction of the medical costs and infrastructure to set a routine examination, especially in the preclinical state of glaucoma, it is necessary to create an alternative method for the early diagnosis of glaucoma.

Glaucoma shows familial aggregation, and its prevalence varies among different ethnic groups (5, 6). This epidemiological evidence strongly suggests that genetic factors play a significant role in the pathogenesis of glaucoma (5, 6). Indeed, previous linkage analyses implicated the genes for myocilin (*MYOC*) (7), optineurin (*OPTN*) (8), and WD-repeat domain 36 (*WDR36*) (9) in the pathogenesis of primary open-angle glaucoma (POAG), the major form of glaucoma. However, further analyses revealed that the frequencies of mutations in these genes were moderate and were associated with POAG in only a small fraction of patients (5). Therefore, the tasks remain to discover authentic and widely associated genetic factors for POAG and to use them for practical diagnostic or medical applications.

To analyze hundreds of thousands of SNPs in a genome-wide association study (GWAS) for POAG, we used DNA chips. This method permits the identification of genetic loci and genes associated with complex human traits, without a priori knowledge of the function or presumptive involvement of any gene in the disease pathway. To date, SNPs associated with over 40 kinds of diseases have been identified (for reviews, see refs. 10, 11). In ocular diseases, an association of lysyl oxidase-like 1 (*LOXL1*) gene polymorphisms with a minor type of secondary glaucoma, exfoliation glaucoma, was recently shown (12). Moreover, SNPs on complement factor H (*CFH*), *C2-CFB*, and a hypothetical gene, *LOC387715*, are associated with the onset of age-related macular degeneration (AMD) (13–15). Although it is still unclear how genes of the systemic immune system are involved in the pathogenesis of a local tissue disease, an additive effect was seen when *CFH* SNPs were combined with SNPs on the other susceptibility genes in predicting the risk for developing AMD (14, 15).

In this study, to identify genetic markers of POAG, we conducted a GWAS in 2 stages at the Kyoto Prefectural University of Medicine using data from a total of 1,575 Japanese POAG patients and control subjects without glaucoma. We obtained a few modestly associated SNPs with POAG belonging to 3 different loci of the genome. The results suggested that the SNPs and the loci identified in this study would be promising genetic markers for the further studies to reveal the molecular mechanism of POAG pathogenesis.

Results

GWAS Stage 1 Analysis. We performed the GWAS for stage 1 by screening 500,568 SNPs to discover genetic markers associated with POAG. We then attempted to reduce the false-positive associations from the results of stage 1 using an independent population in stage 2. Finally, we combined the results of stages 1 and 2 by the Mantel–Haenszel test to evaluate the SNPs identified in this study (Fig. 1). In both stages, we performed

Author contributions: M.K., S.K., and K.T. designed research; M.N., Y.I., T.T., T.Y., M.F., N.O., M.T., S.N., A.M., K.M., and K.T. performed research; M.N., Y.I., T.T., T.Y., M.F., Y.T., K.Y., K.M., S.K., and K.T. analyzed data; and M.N., Y.I., T.T., K.M., S.K., and K.T. wrote the paper.

Conflict of interest statement: This study has been completed under the Collaborative Research Agreement executed by Kyoto Prefectural University of Medicine and Santen Pharmaceutical Co., Ltd. All materials and information produced through this study are the parts of the co-owned intellectual properties. T.T., M.F., and M.K. are employees of Santen Pharmaceutical Co., Ltd.

[1]M.N., Y.I., and T.T. contributed equally to this work.

[2]To whom correspondence may be addressed. E-mail: shigeruk@koto.kpu-m.ac.jp or tashiro@koto.kpu-m.ac.jp.

This article contains supporting information online at www.pnas.org/cgi/content/full/0906397106/DCSupplemental.

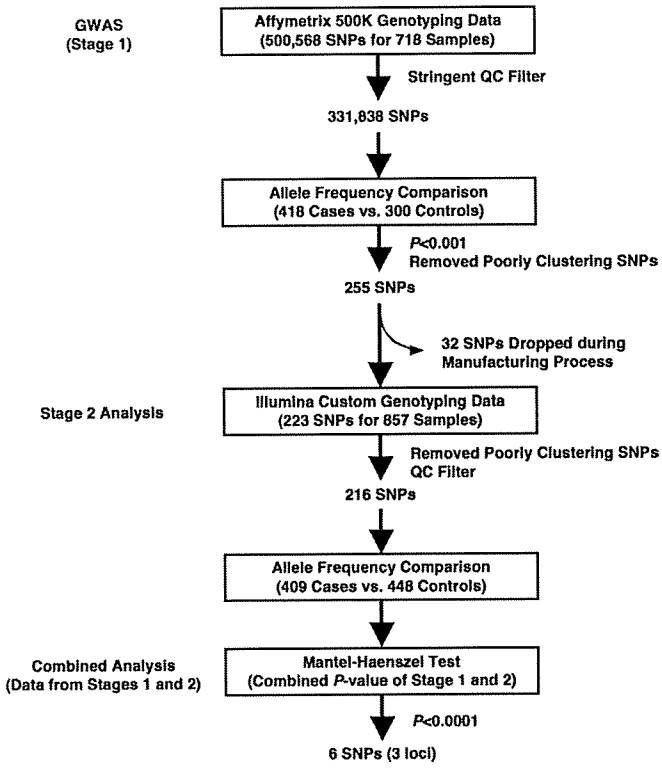

Fig. 1. Project overview for the discovery of genetic markers of POAG. Several hundred SNPs of $P < 0.001$ selected in the GWAS (stage 1) were screened with another study population (stage 2). We identified 6 SNPs of $P < 0.0001$, evaluated by the combined P values of stages 1 and 2 and by the Mantel–Haenszel test. See text for details.

allele frequency comparison to analyze combined P values of stages 1 and 2 by the Mantel–Haenszel test.

Based on our power calculation (see *SI Results* and Fig. S1), we analyzed 718 samples, from 418 POAG patients (case subjects) and 300 control subjects without glaucoma (controls), in stage 1. The clinical characteristics of the study subjects are shown in Table 1. Between the case subjects and controls, no significant difference was observed in gender ratio (female/male: 1.0 vs. 1.3), but a significant difference was observed in their age at the time of blood sampling [64.6 ± 13.5 (n = 418) vs. 51.1 ± 13.9 (n = 300)], which was also seen at the age at diagnosis [58.3 ± 13.4 (n = 324) vs. 51.1 ± 13.9 (n = 300)].

After genotyping the 718 samples, we selected 331,838 SNPs for further analysis, using the stringent criteria chosen for our quality-control (QC) filter (see *SI Results* and Fig. 1). To identify SNPs associated with POAG, we compared the allele frequency of each SNP between case and control samples. In a quantile-quantile plot, the observed P value deviated from the expected P value between $P = 10^{-3}$ and $P = 10^{-4}$. Therefore, we set the threshold at $P = 10^{-3}$ for further analysis (Fig. S2). In total, 431 SNPs showed $P < 0.001$ in the allele frequency comparison (Fig. S2). We then visually checked the 2D cluster plots of these 431 SNPs and selected 255 SNPs as candidates (Fig. 1 and Fig. S3*A*); 176 SNPs were not clearly associated with clusters (Fig. S3*B*). There were no SNPs with significant associations after Bonferroni's correction. Although 1 (rs11056970) of the 255 SNPs in the $10^{-4} < P < 10^{-3}$ group showed a significant deviation ($P < 10^{-10}$) from the Hardy–Weinberg equilibrium (HWE) in the control population, no significant HWE deviation ($P > 10^{-2}$) was observed among the 21 SNPs in the $P < 10^{-4}$ group. We evaluated the SNPs neighboring these 21 SNPs on the 500K array set and found a similar P value ($P = 10^{-3}$-10^{-4}) throughout the linkage disequilibrium (LD) block. These results supported a high confidence in the genotyping results for these SNPs.

Stage 2 Analysis. In stage 2, we analyzed the 255 SNPs of $P < 10^{-3}$ identified in stage 1 that formed good clusters (Fig. 1). To reduce the false-positive associations in stage 1, we used another population of 857 samples, from 409 case subjects and 448 controls, for the stage 2 analysis (see *SI Results*). Because 32 SNPs were dropped during the manufacturing of the custom array, we evaluated the remaining 223 SNPs (Fig. 1).

The clinical characteristics of the 409 POAG patients and 448 control subjects in the stage 2 study are shown in Table 1. In this population, there was a significant difference in the gender ratio in case vs. control subjects (female/male: 1.0:1.8). Although a significant difference was also observed in age at the time of blood sampling [61.9 ± 13.9 (n = 409) vs. 55.2 ± 14.7 (n = 448)], there was no age difference at the time of diagnosis [55.8 ± 13.9 (n = 301) vs. 55.2 ± 14.7 (n = 448)].

Using samples from these subjects, we selected 216 SNPs with high-quality genotyping data from among the 223 SNPs analyzed and used them in the subsequent analysis (Fig. 1).

Combined Analysis of Study Stages 1 and 2. To evaluate the SNPs identified in this study, we compared the allelic frequency of each SNP between case and control samples in stage 2 and calculated their combined P values from stages 1 and 2 by the Mantel–Haenszel test with Yates' correction (Figs. 1 and 2). From the Mantel–Haenszel test, we obtained 6 SNPs with $P < 10^{-4}$ (Fig. 2). Because all these SNPs showed $P < 0.05$ in stage 2 (Table 2), we considered their association to be confirmed

Table 1. Clinical characteristics of case and control samples

	Stage 1			Stage 2		
	Case	Control	*P* value	Case	Control	*P* value
No. subjects participating in case-control analyses	418	300		409	448	
Female/male ratio	1.0 (418)	1.3 (300)	0.17*	1.0 (409)	1.8 (448)	<0.05*
Age (years) at:						
Blood sampling	64.6 ± 13.5 (418)	51.1 ± 13.9† (300)	<0.05‡	61.9 ± 13.9 (409)	55.2 ± 14.7† (448)	<0.05‡
Diagnosis	58.3 ± 13.4 (324)	51.1 ± 13.9† (300)	<0.05‡	55.8 ± 13.9 (301)	55.2 ± 14.7† (448)	0.57‡
Family history of glaucoma, %	26.5 (392)	0 (282)		21.2 (353)	0 (400)	

Numbers in parentheses are the total numbers of subjects whose samples were used for the analysis. Data are indicated as mean ± SD.
*P value of χ^2 test for case and control comparisons.
†Age at blood sampling and diagnosis was the same for the control subjects.
‡P value of Student's t test for case and control comparisons.

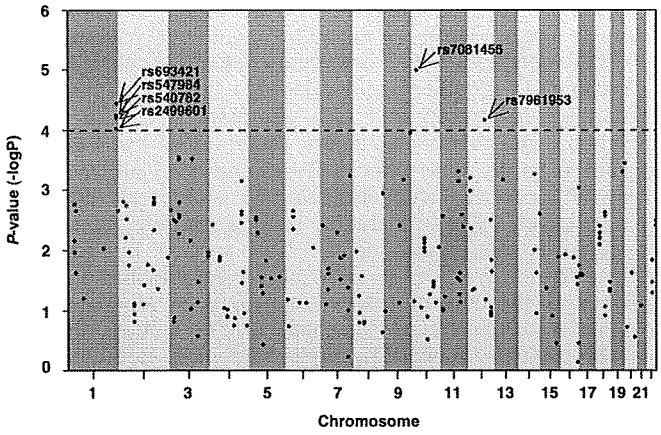

Fig. 2. Distribution of the combined *P* values of stages 1 and 2 calculated by the Mantel–Haenszel test. Comparison of the combined *P* values for allele frequency for 216 SNPs of $P < 0.001$ in stage 1 plotted against chromosomes in numerical order. Horizontal line, $P = 0.0001$ in the Mantel–Haenszel test. Arrows indicate SNPs with $P < 0.0001$.

(Fig. 1). Detailed information about these SNPs is summarized in Table 2 and Table S1. The combined *P* values ranged from 1.0×10^{-5} to 9.0×10^{-5} with an odds ratio (OR) between 1.33 and 1.49 (Table 2). One SNP was intronic, and the others were intergenic (Table 2). Four SNPs (rs547984, rs540782, rs693421, and rs2499601) were located on the same LD block. Although the rs7961953 SNP had a relatively low HWE *P* value ($P = 0.004$) in the stage 2 control group (Table S1), the genotyping data fit the 2D cluster plot (Fig. S3*C*). We evaluated the possible joint contributions of 6 candidate SNPs in a preliminary analysis (Tables S2 and S3 and Fig. S4). We observed that the ORs of the candidate SNPs increased when they were combined (Fig. S4).

The analysis of potential confounding effects by clinical factors such as age, sex, and medical histories showed no significant differences with the genotypes of these 6 candidate SNPs (see *SI Results*), suggesting that the *P* values obtained here were specific results from the case-control comparison.

Population Stratification Analysis. To assess the population heterozygosity, we analyzed the stratification of the populations used in stages 1 and 2. There was no significant difference in population stratification between the case and control subjects of the 2 stages (Fig. S5).

Discussion

In this study, we successfully obtained 6 candidate genetic markers modestly associated with POAG by conducting a GWAS in 2 stages that used independent study populations totaling 1,575 Japanese subjects.

We divided samples from the 1,575 subjects into an initial screening for the GWAS (stage 1) and a stage 2 study (Fig. 1). Because our aim in this study was to identify steady genetic markers of common variants that were significantly associated with the pathogenesis of POAG, we focused on ensuring that the power of our 2-stage association study would be sufficient to detect SNPs possessing reasonably high disease allele frequency and genotype-associated relative risk (Fig. S1). Our design thus resulted in a statistical power sufficient (≥80%) to detect an association with a genotypic relative risk of 2.0 at $P = 1 \times 10^{-7}$ if the disease allele frequency was in the range of 10 to 40%, as long as the number of the samples genotyped in stage 1 exceeded 50% (Fig. S1*A*). For a genotypic relative risk of greater than 1.8, the power was sufficient to detect an association with a disease allele frequency of 0.25 (Fig. S1*B*). In our study, the combined *P* values of the candidate SNPs ranged from 1.0×10^{-5} to 9.0×10^{-5} with the minor allele frequency (MAF) and the respective ORs were between 0.20 and 0.49 or between 1.33 and 1.49 (Table 2). Because the simulated powers were maintained even when we reduced the significance level to $P = 10^{-4}$ (Fig. S1 *C* and *D*), if we regarded a disease allele as a minor allele and assumed that the genotype relative risk was the value of an OR, our sample setting for the 2-stage association study based on the power calculation was ample for our purposes.

In addition to the sample size, statistical power is affected by the accuracy of the clinical data and genotyping results. In our study, 3 ophthalmologists belonging to the same institution selected the POAG patients and control subjects who met our strict criteria so as to reduce any diagnostic variations among the observers. To make certain that our control samples were from volunteers without glaucoma or suspected glaucoma, we performed multiple ophthalmic tests, including a visual field test and fundus examination, for more than 1,100 control volunteers as well as for the POAG patients. To be sure that we excluded samples from volunteers who might be at risk for glaucoma, we preferentially chose volunteers with no evidence of glaucomatous anomalies (category I in case and control selection). Because the prevalence rate of POAG in the Japanese is 3.9% among people older than 40 years of age, as determined by a recent robust epidemiology study called the Tajimi Study (16), volunteers who were 40 years of age or older having a normal diagnosis with a slightly larger cup-to-disc ratio (category II) were considered to have little risk for developing glaucoma, and their samples were included. Finally, we excluded more than 400 volunteers with small optic abnormalities (all category III and some category II) from our study because they did not fit our criteria.

Genotyping errors tend to lead to a false-positive association with a significantly lower *P* value. In our preliminary GWAS analysis, which was done using a standard QC filter (≥85% of call rate per SNP in case and control samples and ≥5% MAF in case and control samples), we observed a large number of SNPs that showed very low *P* values throughout the genome (see

Table 2. List of candidate genetic markers from the Mantel-Haenszel test of SNPs from stages 1 and 2

				Stage 1		Stage 2		Mantel-Haenszel test (stages 1 and 2)	
dbSNP ID	Chr	SNP type	Nearest gene	*P* value	OR (95% CI)	*P* value	OR (95% CI)	*P* value	OR (95% CI)
rs547984	1	Intergenic	*ZP4*	0.00033	1.47 (1.19–1.81)	0.02536	1.24 (1.03–1.50)	0.00006	1.34 (1.16–1.54)
rs540782	1	Intergenic	*ZP4*	0.00037	1.47 (1.19–1.81)	0.02536	1.24 (1.03–1.50)	0.00006	1.34 (1.16–1.54)
rs693421	1	Intergenic	*ZP4*	0.00029	1.48 (1.20–1.83)	0.01839	1.26 (1.04–1.52)	0.00004	1.35 (1.17–1.56)
rs2499601	1	Intergenic	*ZP4*	0.00058	1.45 (1.17–1.79)	0.02679	1.24 (1.02–1.50)	0.00009	1.33 (1.15–1.53)
rs7081455	10	Intergenic	*PLXDC2*	0.00005	1.70 (1.31–2.19)	0.02005	1.33 (1.05–1.69)	0.00001	1.49 (1.25–1.77)
rs7961953	12	Intronic	*DKFZp762A217*	0.00096	1.48 (1.17–1.86)	0.01482	1.30 (1.05–1.60)	0.00007	1.37 (1.18–1.61)

P values are for allele frequency comparison between case and control. Chr, chromosome; CI, confidence interval.

SI Results and Fig. S6*A*). When we analyzed the data precisely, we found that hundreds of high-ranked SNPs showed both a significantly low call rate (Fig. S6*B*) and a large difference in call rate between the case and control samples (Fig. S6*C*). Most of these SNPs showed obvious genotyping errors and poor clustering (Figs. S6 *D* and *E*). Therefore, we adopted our stringent QC filter to remove such low-quality data and carefully checked the 2D cluster plots in both stages 1 and 2, even after applying the QC filter (Fig. 1). Using our stringent filter, the genotype concordance after extracting high-quality data from the different genotyping systems used in stages 1 and 2 was 99.8%. We verified this by genotyping 216 SNPs using 104 samples (52 control and 52 case samples) by both genotyping methods (see *SI Results*). This result supports a high confidence value for the genotyping data that we obtained after QC filtering and visual checking of the 2D cluster plots.

More recently, Yamaguchi-Kabata et al. (17) reported that Japanese population stratification could mainly be divided into 2 clusters: the main islands of Hondo and Ryukyu from Okinawa. They suggested that the false-positive rates in GWASs would be acceptable when the samples were collected from Hondo in Japan, indicating that the population stratification within the region was relatively small. In this study, we collected all the samples at a single institution in the middle part of Hondo. As expected, we observed no obvious population stratification between case and control samples in stages 1 and 2 (Fig. S5). These data indicated that *P* values obtained here were specific results from the case-control comparison.

Thus, beginning with stringent diagnostic criteria, we successfully used our polished genotype data to obtain 6 candidate genetic markers that were modestly associated with POAG. Because 4 SNPs (rs547984, rs540782, rs693421, and rs2499601) showed a strong LD with each other, we ultimately obtained 3 genetic loci associated with a potential functional determinant of POAG pathogenesis. Interestingly, of these 3 loci, none was associated with the previously reported associated genes *MYOC* (7), *OPTN* (8), and *WDR36* (9). Under our conditions, all the SNPs associated with these genes were dropped in stage 1 because they did not pass the $P < 10^{-3}$ filter. *P* values of 6 candidate SNPs in stage 2 were not so low when compared with those in stage 1 (Table 2). Slight difference, such as the ratio of classic POAG and normal tension glaucoma (NTG) subtypes, between the population of stages 1 and 2 might affect the differences of these *P* values.

To evaluate the 3 genetic loci that we determined to be associated with POAG, we performed high-density genotyping around the SNP (rs7081455) that showed the highest association in our study. Although we obtained a POAG-associated SNP (allele frequency comparison, $P < 0.05$) on the same LD block, we were still not able to link the SNP to the annotated gene(s).

Recently, Thorleifsson et al. (12) performed a GWAS and demonstrated that 3 SNPs on *LOXL1* are strongly associated with exfoliation glaucoma, which is one of the fewer types of open-angle glaucoma compared to the POAG, in 2 populations of subjects from Iceland and Sweden. Although the risk haplotype differs with different populations, a strong association between the SNPs on *LOXL1* and exfoliation glaucoma has been replicated in many studies (18–26), including ours of Japanese subjects (27), even when the sample size was relatively small. However, in our GWAS, in which the power was sufficient to detect SNPs with a high genotype risk ratio (Fig. S1), none of the SNPs was adjacent to *LOXL1*. Our data thus indicate that POAG may be more complicated than exfoliation glaucoma, because multiple SNPs with a moderate OR appear to be involved in its pathogenesis.

POAG manifests as 2 subtypes: POAG with high intraocular pressure (IOP; classic POAG subtype) and POAG with normal IOP (NTG subtype). Because the clinical states of both subtypes overlap almost completely, they are usually categorized as a single disease. However, most Japanese POAG patients have the NTG subtype, which is a unique epidemiological distribution, compared with other populations (16). Previous reports showed that toll-like receptor 4 (28) was associated with the NTG subtype and that NCK adaptor protein 2 (29) was the nearest gene from the locus associated with the NTG subtype revealed by the association study using an SNP or microsatellite marker, respectively. These 2 studies were attempting to reveal the molecular mechanism of the NTG-specific pathogenesis by focusing on a gene or locus based on previous knowledge, whereas the current study design aims to identify causative gene(s) for the common mechanism of both classic POAG and NTG subtypes by whole-genome screening. Because we combined the patients from both subtypes as a single case group to obtain a larger sample size, the genetic loci identified in this study are most likely to be components of the molecular mechanism underlying a particular neurodegenerative pathway. If we divided the samples into the classic POAG and NTG subtypes and carried out separate GWASs with enough power to detect associations, we might be able to identify genetic loci or molecule(s) that are associated with mechanisms of pathogenesis and/or progression specific to the NTG subtype, such as the genes described in the previous reports (28, 29), at least some of which would probably be related to the control of IOP.

In this study, we obtained 6 candidate SNPs located on the 3 different loci that are modestly associated with the pathogenesis of POAG. This conclusion was achievable only because we used (*i*) an adequate distribution of the limited subjects available in the 2-stage association study, based on the power simulation; (*ii*) stringent diagnostic criteria to distinguish clearly between POAG patients and control subjects without glaucoma; and (*iii*) a stringent data filter along with a careful visual check of the 2D cluster plots so as to restrict the genotyping data to a meaningful subset. However, we could not link these SNPs and their surroundings within the 3 loci to specific gene(s), which might have helped us to elucidate the molecular mechanism of POAG pathogenesis. It is also worth noting that other loci associated with POAG may have been dropped from this study, owing to the impaired SNP density caused by the stringent QC filter and/or because some are latent rare variants that could not be detected at all by the current study design. Along with the 3 loci discovered in this study, the identification of loci we missed, by performing large-scale association studies, replication study using an independent cohort, and subsequent in-depth sequencing, could provide a complete set of genetic markers useful for diagnosing POAG as well as for revealing the molecular mechanism of its pathogenesis.

Materials and Methods

Case and Control Subjects. ***Enrollment of participants and blood sampling.*** All procedures were conducted in accordance with the Helsinki Declaration. This study was approved by the Institutional Review Board of Kyoto Prefectural University of Medicine. All participants provided written informed consent after an explanation of the nature and possible consequences of the study, and they were interviewed to determine their familial history of glaucoma and other ocular or general diseases. A total of 1,591 Japanese participants were recruited to give peripheral blood samples for this study between March 2005 and December 2007. Because 16 of the 1,591 sets of genotyping data were dropped during the genotyping process (see *SI Text*), the data derived from 1,575 participants were used. Blood samples were assigned an anonymous code by a third person who was blinded to both the blood sampling and genotyping. Genomic DNA was isolated from the blood, and Epstein-Barr virus–transformed lymphocytes were prepared to serve as a future resource of genomic DNA (see *SI Text*).

Selection of case subjects and control subjects. We recruited the case patients with POAG and control subjects without glaucoma for this study at the University Hospital of Kyoto Prefectural University of Medicine (Kyoto, Japan). Both the case and control groups in stages 1 and 2 received the following serial ophthalmic examinations for diagnosis: silt-lamp and fundus examination,

gonioscopy, visual field tests, and IOP measurements. The anterior chamber angle was examined by means of a slit-lamp, based on the method of van Herick et al. (30). The ocular fundus was examined using a confocal scanning laser ophthalmoscope (HRT-II; Heidelberg Engineering GmbH), scanning laser polarimeter (GDx-VCC; Carl Zeiss Meditec), and fundus photography (TRC-NW200; Topcon). The visual field was tested by frequency-doubling technology perimetry (Matrix; Carl Zeiss Meditec) using program N-30/Humphrey automated perimetry with program 30–2 SITA Fast and/or Standard (Carl Zeiss Meditec) and/or Goldmann perimetry (Haag–Streit) for both study groups. The IOP was measured by a noncontact tonometer (RKT-7700; Nidek) for the selection of control subjects and by a Goldmann applanation tonometer (Haag–Streit) for both study groups. Three ophthalmologists (Y.I., S.K., and K.M.) diagnosed glaucoma in the patients, based on the diagnosis standard (31). The baseline IOPs of case groups in stages 1 and 2 were 15.5 ± 3.9 mmHg (mean ± SD, $n = 157$) and 15.5 ± 3.1 mmHg (mean ± SD, $n = 154$), respectively, whereas the mean deviations of Humphrey perimetry were −10.7 ± 8.6 dB ($n = 319$) and −10.1 ± 8.1 dB ($n = 261$), respectively. We could not obtain all the cases' baseline IOP or mean deviation of visual field data because of the severity of the disease. Further information for selecting case and control subjects is detailed in *SI Text*.

GWAS (Stage 1). ***SNP genotyping.*** We first genotyped the whole-genome SNPs of 425 case and 301 control samples on an Affymetrix GeneChip Mapping 500K Array Set, following the manufacturer's instructions. The protocols for obtaining SNP data are described in *SI Text*.

Criteria for SNP selection. From 500,568 SNPs (262,264 and 238,304 SNPs in the Nsp I and Styl arrays, respectively), a total of 331,838 autosomal SNPs were selected for association analysis based on our stringent QC filter, which had the following criteria: (*i*) ≥90% call rate per SNP in case and control samples, (*ii*) ≤5% call rate difference between case and control samples for each SNP, and (*iii*) ≥5% MAF in case and control samples. After the association analysis, we visually checked the 2D cluster plots of the genotypes for each $P < 10^{-3}$-ranked SNP (431 SNPs) to remove SNPs that clustered poorly. The scoring system for assessing the 2D cluster plots is detailed in *SI Text*. We finally selected 255 SNPs as the stage 1 candidates.

Stage 2 Analysis. ***SNP genotyping.*** We next attempted to replicate the genotyping of the 255 candidate SNPs identified in stage 1 using samples from another population of 410 case subjects and 455 control subjects by means of the iSelect Custom Infinium Genotyping system (Illumina). The protocols for obtaining SNP data are described in *SI Text*.

Criteria for SNP selection. From the 223 SNPs, a total of 216 SNPs were selected for the association analysis based on our QC filter: (*i*) ≥90% of call rate per SNP for both case and control, respectively, and (*ii*) ≥5% of MAF for both case and control. To validate the genotyping accuracy in stages 1 and 2, we genotyped the 216 SNPs in 104 (52 case and 52 control) samples using both an Affymetrix 500K Array Set and the iSelect system and analyzed the genotype concordance between the 2 systems (see *SI Text*).

Population Stratification. To analyze the stratification of our stage 1 and 2 populations, we used STRUCTURE version 2.2 software (http://pritch.bsd.uchicago.edu/software.html). Detailed protocols are described in *SI Text*.

Statistical Analysis. To manage all the genotyped data, we used LaboServer (World Fusion Co., Ltd.) as a laboratory information management system. We used LaboServer, Microsoft Office Excel 2003 (Microsoft), and R for the statistical analysis. The power calculation was performed using CaTS software (www.sph.umich.edu/csg/abecasis/CaTS/index.html) (see *SI Text*).

The frequency of alleles in case and control samples was compared using the basic allele test. The OR and the upper and lower limits of the 95% confidence interval of each SNP were calculated for the allele possessing a higher frequency in the case samples than in the control samples. The HWE was evaluated by the χ^2 test. Quantile–quantile plots were generated by ranking the observed values from minimum to maximum and plotting them against their expected values (32). To examine the possible confounding effects of several factors, such as age, gender, history of systemic disease, and reported risk of glaucoma, we assessed the correlations between the clinical profile values and the genotype data from the case and control samples by one-way ANOVA or χ^2 test (33, 34). The Mantel–Haenszel test with Yates' correction was performed as described previously (35). All the numerical data were expressed as the mean ± SD.

ACKNOWLEDGMENTS. We thank all the patients and volunteers who enrolled in our study. We also thank Ms. Sayaka Ohashi, Ms. Naoko Saito, and Ms. Yuko Konoshima for processing blood samples and performing genotyping; Mrs. Hiromi Yamada, Ms. Aiko Hashimoto, Ms. Keiko Nirasawa, and Mrs. Akemi Tanaka for their assistance in clinical information analysis; Mr. Ryuichi Sato and Ms. Fumiko Sato (World Fusion, Tokyo, Japan) for management of the genotype data; Mr. Hiroshi Inoue for the logistic regression analysis and excellent advice regarding statistical analysis; and Ms. Tomoko Tsuda for excellent secretarial assistance. This work was supported by grants from the Collaborative Development of Innovative Seeds of the Japan Science and Technology Agency (M.K. and K.T.); Ministry of Health, Labor, and Welfare of Japan (K.M., S.K. and K.T.), and Santen Pharmaceutical Co., Ltd (S.K. and K.T).

1. Quigley HA, Broman AT (2006) The number of people with glaucoma worldwide in 2010 and 2020. *Br J Ophthalmol* 90:262–267.
2. Heijl A, et al. (2002) Reduction of intraocular pressure and glaucoma progression: Results from the Early Manifest Glaucoma Trial. *Arch Ophthalmol* 120:1268–1279.
3. Leske MC, et al. (2003) Factors for glaucoma progression and the effect of treatment: The Early Manifest Glaucoma Trial. *Arch Ophthalmol* 121:48–56.
4. Leske MC, Heijl A, Hyman L, Bengtsson B (1999) Early Manifest Glaucoma Trial: Design and baseline data. *Ophthalmology* 106:2144–2153.
5. Hewitt AW, Craig JE, Mackey DA (2006) Complex genetics of complex traits: The case of primary open-angle glaucoma. *Clin Exp Ophthalmol* 34:472–484.
6. Fan BJ, Wang DY, Lam DS, Pang CP (2006) Gene mapping for primary open angle glaucoma. *Clin Biochem* 39:249–258.
7. Stone EM, et al. (1997) Identification of a gene that causes primary open angle glaucoma. *Science* 275:668–670.
8. Rezaie T, et al. (2002) Adult-onset primary open-angle glaucoma caused by mutations in optineurin. *Science* 295:1077–1079.
9. Monemi S, et al. (2005) Identification of a novel adult-onset primary open-angle glaucoma (POAG) gene on 5q22.1. *Hum Mol Genet* 14:725–733.
10. Topol EJ, Murray SS, Frazer KA (2007) The genomics gold rush. *J Am Med Assoc* 298:218–221.
11. Kingsmore SF, Lindquist IE, Mudge J, Gessler DD, Beavis WD (2008) Genome-wide association studies: Progress and potential for drug discovery and development. *Nat Rev Drug Discovery* 7:221–230.
12. Thorleifsson G, et al. (2007) Common sequence variants in the LOXL1 gene confer susceptibility to exfoliation glaucoma. *Science* 317:1397–1400.
13. Klein RJ, et al. (2005) Complement factor H polymorphism in age-related macular degeneration. *Science* 308:385–389.
14. Maller J, et al. (2006) Common variation in three genes, including a noncoding variant in CFH, strongly influences risk of age-related macular degeneration. *Nat Genet* 38:1055–1059.
15. Ross RJ, et al. (2007) Genetic markers and biomarkers for age-related macular degeneration. *Expert Rev Ophthalmol* 2:443–457.
16. Iwase A, et al. (2004) The prevalence of primary open-angle glaucoma in Japanese: The Tajimi Study. *Ophthalmology* 111:1641–1648.
17. Yamaguchi-Kabata Y, et al. (2008) Japanese population structure, based on SNP genotypes from 7003 individuals compared to other ethnic groups: Effects on population-based association studies. *Am J Hum Genet* 83:445–456.
18. Aragon-Martin JA, et al. (2008) Evaluation of LOXL1 gene polymorphisms in exfoliation syndrome and exfoliation glaucoma. *Mol Vis* 14:533–541.
19. Challa P, et al. (2008) Analysis of LOXL1 polymorphisms in a United States population with pseudoexfoliation glaucoma. *Mol Vis* 14:146–149.
20. Fan BJ, et al. (2008) DNA sequence variants in the LOXL1 gene are associated with pseudoexfoliation glaucoma in a U.S. clinic-based population with broad ethnic diversity. *BMC Med Genet* 9:5.
21. Fingert JH, et al. (2007) LOXL1 mutations are associated with exfoliation syndrome in patients from the midwestern United States. *Am J Ophthalmol* 144:974–975.
22. Hayashi H, Gotoh N, Ueda Y, Nakanishi H, Yoshimura N (2008) Lysyl oxidase-like 1 polymorphisms and exfoliation syndrome in the Japanese population. *Am J Ophthalmol* 145:582–585.
23. Mossbock G, et al. (2008) Lysyl oxidase-like protein 1 (LOXL1) gene polymorphisms and exfoliation glaucoma in a Central European population. *Mol Vis* 14:857–861.
24. Ozaki M, et al. (2008) Association of LOXL1 gene polymorphisms with pseudoexfoliation in the Japanese. *Invest Ophthalmol Vis Sci* 49:3976–3980.
25. Pasutto F, et al. (2008) Association of LOXL1 common sequence variants in German and Italian patients with pseudoexfoliation syndrome and pseudoexfoliation glaucoma. *Invest Ophthalmol Vis Sci* 49:1459–1463.
26. Yang X, et al. (2008) Genetic association of LOXL1 gene variants and exfoliation glaucoma in a Utah cohort. *Cell Cycle* 7:521–524.
27. Mori K, et al. (2008) LOXL1 genetic polymorphisms are associated with exfoliation glaucoma in the Japanese population. *Mol Vis* 14:1037–1040.
28. Shibuya E, et al. (2008) Association of toll-like receptor 4 gene polymorphisms with normal tension glaucoma. *Invest Ophthalmol Vis Sci* 49:4453–4457.
29. Akiyama M, et al. (2008) Microsatellite analysis of the GLC1B locus on chromosome 2 points to NCK2 as a new candidate gene for normal tension glaucoma. *Br J Ophthalmol* 92:1293–1296.
30. Van Herick W, Schwartz A (1969) Estimation of width of angle of anterior chamber incidence and significance of the narrow angle. *Am J Ophthalmol* 68:626–629.
31. European Glaucoma Society (2003) *Terminology and Guidelines for Glaucoma* (Dogma, Savona, Italy), 2nd Ed, pp 1–152.
32. Balding DJ (2006) A tutorial on statistical methods for population association studies. *Nat Rev Genet* 7:781–791.
33. Miyamoto Y, et al. (2007) A functional polymorphism in the 5′ UTR of GDF5 is associated with susceptibility to osteoarthritis. *Nat Genet* 39:529–533.
34. Ozaki K, et al. (2006) A functional SNP in PSMA6 confers risk of myocardial infarction in the Japanese population. *Nat Genet* 38:921–925.
35. Mantel N, Haenszel W (1959) Statistical aspects of the analysis of data from retrospective studies of disease. *J Natl Cancer Inst* 22:719–748.

Supporting Information

Nakano et al. 10.1073/pnas.0906397106

SI Text

SI Results

Family History of Glaucoma. In the enrollment interview, 26.5 and 21.2% of our POAG subjects in stages 1 and 2, respectively, declared a family history of some type of glaucoma (Table 1). The control volunteers all stated that they had no family history of glaucoma (Table 1).

Statistical Power Estimate. To design an effective study using a total of 1,575 patients and control subjects for a GWAS (stage 1) and stage 2 analysis, we first used CaTS software to simulate the division of samples into the 2 stages (see *SI Materials and Methods*). When we set the significance level at 1×10^{-7}, which usually corresponds to the level of Bonferroni's correction in GWASs that use 500K chips, the statistical power was saturated at 50% of the samples in stage 1 when changing the value of either the disease allele frequency (Fig. S1*A*) or the genotype relative risk (Fig. S1*B*). Therefore, we decided to split our samples approximately in half for stages 1 and 2.

Genotyping for GWAS (Stage 1). We first genotyped 425 case and 301 control samples using the Affymetrix GeneChip Mapping 500K Array Set. According to the genotyping data by dynamic model (DM) algorithm, we found no mixed-up samples between Nsp I and StyI arrays. We observed inconsistent results for gender between the clinical records and the genotyping results in 4 case samples. The genotyping concordance measured by using 4 samples in duplicate was 99.5 ± 0.1% and 99.5 ± 0.2% on the Nsp I and StyI arrays, respectively.

The final genotyping results for 500,568 SNPs of the 500K array set were called by the Bayesian robust linear model with a Mahalanobis distance classifier (BRLMM) algorithm. The value of the cluster distance or raw intensity of 3 case samples and 1 control sample, respectively, were out of the accepted range. In total, 7 case samples and 1 control sample with gender mismatch and/or low-quality data were excluded from the analysis. Ultimately, we used 418 cases and 300 controls for the association study. The mean call rate per sample was 98.3 ± 0.9% and 98.4 ± 1.1% for the case and control samples, respectively. Our stringent QC filter for the call rate and MAF (see *Materials and Methods*) permitted 331,838 autosomal SNPs to be used in the subsequent analysis (Fig. 1).

Genotyping for Stage 2 Analysis. We first genotyped the SNPs identified in stage 1 in samples from a separate population of 410 case and 455 control subjects. After reprocessing the samples with a lower call rate (see *Materials and Methods*), we excluded data from 1 case subject with exfoliative glaucoma and 6 control subjects who were related to each other. We also excluded 1 control sample for which the gender was inconsistent between the clinical records and genotyping results. Our final sample set for the association analysis totaled 857, from 409 case and 448 control subjects. The mean call rate per sample was 98.2 ± 0.1% for both the case and control samples, after a visual check of the 2D cluster plots (Fig. S3 *C–F*) and elimination of poorly clustered SNPs. Using the QC filter (see *SI Materials and Methods*), we selected 216 SNPs for the combined analysis (Fig. 1). To validate the genotyping accuracy between the Affymetrix GeneChip and Illumina iSelect systems, we compared the genotype results for the 216 SNPs of 104 samples (52 case and 52 control samples). The genotype concordance between the 2 systems was 99.8%.

Preliminary Analysis of Joint Contribution of Candidate SNPs. We performed logistic regression analysis to evaluate the possible joint contributions of 3 SNPs (rs547984, rs7081455, and rs7961953) from among the 6 candidate SNPs. Table S2 shows the Akaike's information criterion (AIC) for various genetic models with or without interactions for all the combinations among these SNPs. An additive model without interaction was the best-fit model for each factor (Table S2), and the 3-factor model showed the lowest AIC (Table S3). The joint ORs relative to that of the lowest risk genotype for the SNP combination were then calculated to estimate the combined effects of the SNPs. When we combined all 3 SNPs, some values appeared to be unreliable because of a small number of individuals in some of the genotype combinations; therefore, we paired the SNPs for analysis. The joint ORs of every possible pair among the 3 SNPs increased from that of a single SNP, 1.8–2.0, to 2.4–3.0, which correlated with the risk value for the corresponding allele (Fig. S4). These results suggested that a combination of the candidate SNPs from this study would probably be useful as genetic markers for predicting the risk of developing POAG.

Analysis of Population Stratification. To analyze the population stratification for stages 1 and 2, we used STRUCTURE version 2.2 software (http://pritch.bsd.uchicago.edu/software.html). We extracted the unlinked SNP set from stages 1 and 2 and ran the program for 100,000 burn-in steps, followed by 300,000 Markov Chain Monte Carlo steps from K (assumed population number) = 1–5 (see *Materials and Methods*). Our case plus control samples showed a similar stratification with those of HapMap-JPT (Fig. S5 *A* and *C*) and clearly differed from those of HapMap-CEU and -YRI (Fig. S5*A* and *C*). This analysis showed no significant difference in population stratification between the case and control samples used in stages 1 and 2 (Fig. S5 *B* and *D*).

Assessment of Confounding Effects. After the combined analysis of stages 1 and 2 by the Mantel–Haenszel test (Table 2), we assessed the correlations between the clinical profiles and the genotype data for the stage 1 plus 2 subjects to examine the potentially confounding effects of age, gender, history of systemic diseases, and reported risk factors for glaucoma. In the combined populations, a comparison showed 8 of 11 clinical profiles with $P < 0.05$ between case subjects and control subjects (Table S4). We evaluated the correlations between these 8 clinical profiles and the genotypes of the 6 candidate SNPs (Table S5). Although 4 correlations (rs547984, rs540782, rs693421, and rs2499601) were found ($P < 0.05$) for patients with diabetes mellitus in the case group (Table S5), none was statistically significant after using Bonferroni's correction (1).

Preliminary GWAS with a Standard Filter. In our preliminary GWAS, a standard filter (i.e., ≥85% call rate per SNP and ≥5% MAF in case and control samples) was used, and the allele frequency between case and control data was compared (Fig. S6*A*). Using this filter, we found an enormous number of SNPs with a low P value throughout the genome (Fig. S6*A*). We also observed a significantly lower call rate of high-ranked SNPs with low P values (Fig. S6*B*), compared with that of our stringent QC filter, and a large difference in the call rate between case and

control samples (Fig. S6*C*). Most of these high-ranked SNPs showed obvious genotyping errors and were not in tight clusters (Fig. S6 *D* and *E*).

SI Discussion

We assessed the joint contributions of the SNPs discovered in this study. We found that the 3 candidate SNPs independently contributed to the disease and that the combination of all 3 SNPs showed the best fit in a logistic regression analysis (Tables S2 and S3). Moreover, the joint ORs of these SNPs increased with the number of risk alleles when they were assessed in combination (Fig. S4). These results demonstrated that the risk for POAG increased with an increased number of these SNPs, located at different genomic loci, which also meant that multiple genetic factors are probably involved in the pathogenesis of POAG. In the case of AMD, Maller et al. (2) demonstrated that AMD-associated SNPs were not only related to *CFH* but to other susceptibility genes located at different chromosomal loci and that they had a joint effect, with a marked increase in relative risk. Their results supported the idea that these genetic markers might facilitate the diagnosis of AMD. Our set of candidate SNPs is likewise a promising tool for the diagnosis of POAG, which would help in preventing visual loss by prompting early medical intervention.

SI Materials and Methods

Genomic DNA. Genomic DNA was isolated from 350 μL of peripheral blood by means of a BioRobot EZ1 (Qiagen) using the EZ1 DNA Blood 350-μL Mini Kit (Qiagen), according to the manufacturer's instructions. The amount and quality of the isolated DNA were analyzed using an UV spectrophotometer (NanoDrop; NanoDrop Technologies) and agarose gel electrophoresis. Genomic DNA was stored at −80 °C until use.

Preparation of Epstein–Barr Virus (EBV)-Transformed Lymphocytes. Lymphocytes prepared from the blood were transformed with EBV from the supernatant of B95–8 (JCRB9123; Health Science Research Resources Bank, Japan) as reported previously (3) and cultured for 2 weeks to enrich for EBV-transformed lymphocytes. The cells were then stored in liquid nitrogen as a future source of genomic DNA.

Management of Clinical Information. All participants were interviewed to obtain their general clinical profile, including their family history of glaucoma and other ocular or general diseases. Clinical profiles from the interview and data collected during the ophthalmic examinations were recorded using FileMaker Pro 5.5 database software (FileMaker, Inc.). The data were then transferred to Kiroku data management software (World Fusion Co., Ltd.), and an anonymous code was assigned to the data for later comparison with the genotyping data from the association analysis. These data were managed by the same person who assigned the anonymous code to the blood samples.

Database. All the genomic data presented in this article, such as the physical position of the chromosome, SNP identification number, and gene annotation, were based on the National Center for Biotechnology Information Build 35, Human Genome Assembly.

Selection of Case Subjects and Control Subjects. Three ophthalmologists (Y.I., S.K., and K.M.) diagnosed glaucoma in the patients, based on the diagnosis standard (4). In brief, the criteria for POAG with high IOP (classic POAG subtype) were (*i*) glaucomatous defect corresponding to optic disc damage in the visual field with compatible optic nerve cupping and retinal nerve fiber-layer defect (NFLD) or notching, (*ii*) open anterior chamber angle on gonioscopy, (*iii*) a maximum IOP of more than 21 mmHg without treatment, and (*iv*) no history or signs of other eye diseases. For POAG with normal IOP (NTG subtype), the criteria were identical to those for classic POAG, except that the maximum IOP was equal to or less than 21 mmHg without treatment. Patients whose glaucoma could not be categorized as a POAG subtype (e.g., exfoliative glaucoma, pigmentary glaucoma, steroid-induced glaucoma, neovascular glaucoma, primary angle closure glaucoma) were excluded from this study. From the pool of patients tested, we selected 835 POAG patients as a case group. We used samples from 425 of these patients in the GWAS (stage 1) and from 410 patients in the stage 2 analysis.

The volunteers who were selected as control subjects were carefully examined for glaucoma or suspected glaucoma, as reported previously (5), by the same 3 ophthalmologists. If the control volunteers had representative visual field defects of at least 1 abnormal test point after the additional frequency-doubling technology testing, they were tested by Humphrey automated perimetry with the program 30-2 SITA Fast (Carl Zeiss Meditec). If the control volunteers had an IOP more than 21 mmHg with a noncontact tonometer, they were remeasured using a Goldmann applanation tonometer. If the control volunteers had a narrow angle equal to grade 2 or less using the system developed by van Herick et al. (6), this finding was confirmed using gonioscopy. Additionally, volunteers without glaucoma who passed the previously discussed examinations were subdivided into 3 categories (categories I–III). In category I, the vertical cup-to-disc (C/D) ratio was within 0.6 without any NFLD, notching, bayoneting, or undermining. In category II, the vertical C/D ratio was within 0.7 without any NFLD or notching. In category III, the visual field was within normal limits, but a thin NFLD or small notch was observed or the vertical C/D ratio was over 0.7. In all the categories, the color of the rim was good and no visual field loss was observed. Of the control volunteers assigned to category II, we selected only subjects who were 40 or more years of age at the time of blood sampling. Our final control group consisted of 756 volunteers without glaucoma [569 from category I and 187 from category II ($\geq$40 years old)] and without a family history of glaucoma. Of these volunteers, we used samples from 301 for stage 1 and samples from 455 for stage 2.

Power Calculation. The power calculation was performed by using CaTS software with the following conditions: sample size, 800 case and 800 control samples; markers genotyped in stage 2, 0.1% (500/500,000 SNPs); significance level, 1×10^{-7} (0.05/500,000) and 1×10^{-4}; prevalence of POAG, 0.039 according to the epidemiological study carried out in Japan (5); and genetic model, additive. The power of the joint analysis to consider how many samples should be allocated to stage 1 or 2 was then calculated by changing the value of either the disease allele frequency or the genotype risk ratio.

Sample Preparation, Array Hybridization, Scanning, and Genotyping in Stage 1. We genotyped the whole-genome SNPs of 425 case and 301 control samples using the Affymetrix GeneChip Mapping 500K Array Set, according to the manufacturer's instructions. In brief, 2 aliquots of $\approx$250 ng of genomic DNA were digested with either NspI or StyI (New England Biolabs) for 2 h at 37 °C. Adaptor oligonucleotides specific to each digested end were then ligated with T4 DNA Ligase (New England Biolabs) for 3 h at 16 °C. After dilution with water, the ligated products were divided into 3 aliquots and amplified by PCR using Titanium TaqDNA polymerase (BD Biosciences) in the presence of adaptor-specific primers (PCR primer, 002; Affymetrix), dNTP (Takara), and GC-Melt Reagent (Clontech). The PCR conditions were an initial denaturation of 94 °C for 3 min; 30 cycles of denaturation at 94 °C for 30 sec, annealing at 60 °C for 30 sec, extension at 68 °C for 15 sec; and a final extension for 7 min. The PCR products from the 3 reactions were combined and subse-

quently purified by using the NucleoFast 96 PCR Plate (Clontech). The purified PCR products were then fragmented by DNase I (Affymetrix) at 37 °C for 35 min. The fragmentation was analyzed by 2% weight/volume agarose gel electrophoresis and/or a multicapillary electrophoresis system (HDA-GT12; eGene) with a Gel Cartridge Kit-F (eGene). The fragmented products were denatured and end-labeled by GeneChip DNA Labeling Reagent (Affymetrix) using terminal deoxynucleotidyl transferase (Affymetrix) at 37 °C for 4 h. The labeled products were then hybridized onto the corresponding Nsp I or StyI array. Following hybridization at 49 °C for 16–18 h, the arrays were washed and stained by incubating them with biotinylated anti-streptavidin antibody (Vector Laboratories) and streptavidin-phycoerythrin (Invitrogen) using the GeneChip Fluidics Station 450 (Affymetrix). The stained arrays were scanned by a GeneChip Scanner 3000 (Affymetrix). The scan data were managed by the GeneChip Operating Software (Affymetrix). The intensity data provided by the CEL files were used for SNP genotyping as described below.

To check the quality of each array, the SNPs were initially genotyped by a DM algorithm using GeneChip Genotyping Analysis Software (Affymetrix). The DM algorithm calls the genotype of each SNP by judging 3 patterns (AA, AB, and BB genotypes) based on the intensity data from each probe on the array. Arrays that did not pass a call rate of 93% at a confidence threshold of 0.33 were rehybridized using the stored hybridization mixture. Because 46 and 40 arrays for NspI and StyI, respectively, still did not pass the 93% call rate, we used only the data with the higher call. To confirm that no samples were mixed up, we checked the genotypes of 50 common SNPs placed on both the Nsp I and StyI arrays. We also checked for gender mismatch by comparing clinical records and genotyping results for the X-chromosome. The reproducibility of our genotyping in this system was confirmed by the processing of 4 samples in duplicate (see *SI Results*).

For the association analysis, we genotyped the SNPs by the BRLMM algorithm using a BRLMM Analysis Tool (Affymetrix). The BRLMM algorithm is a significant improvement over the DM algorithm for raising the call rate and accuracy and for obtaining a balanced performance between homozygotes and heterozygotes. These improved performances are achieved by using a multiple-array method that corrects the probe-specific effects and genotypes by a multiple-sample classification with the initial prediction by DM. The multiple-sample classification was performed by clustering 425 case samples and 301 control samples. After excluding 8 samples with gender mismatch and/or low-quality data (see *SI Results*), we used 418 case and 300 control samples for the association analysis. After the association analysis, we also extracted the neighboring SNPs of the most highly ranked candidate SNPs ($P < 10^{-4}$), based on the LD block of the HapMap-JPT and -CHB populations derived from the UCSC Genome Browser (University of California Santa Cruz; http://genome.ucsc.edu/cgi-bin/hgGateway) to evaluate the genotyping confidence for these SNPs in stage 2.

We adopted the scoring system to assess the 2D cluster plots of genotyping results. Using our custom tool, we first selected 300 SNPs with good 2D cluster plots, as described below. The cluster for each SNP was given an acceptability score (0, reject; 1, acceptable; and 2, accept), and this was done separately for the case and control data. The clusters were scored in random order by 3 independent observers (M.N., T.T., and K.T.). To be accepted, the score given by at least 2 observers had to agree, and it was expressed as a total acceptability score of the summed case and control scores, ranging from 0 to 4. We excluded poorly clustered SNPs, which were given a total score of 0 to 2. We carefully compared the 2D cluster plots of SNPs that showed a score of 3 against the *P* values of their surrounding SNPs and their LD block. When the *P* values of the "score 3" SNPs and the surrounding SNPs were extremely different, we excluded the SNPs as a genotyping error. We also had different observers (Y.T., M.F., and T.Y.) re-examine the 2D cluster plots of the initially selected 300 SNPs using the SnpSignalTool 1.0.0.12 (Affymetrix) as described previously.

Sample Preparation, Array Hybridization, and Scanning in Stage 2. We analyzed 255 candidate SNPs identified in stage 1 using another set of 410 case subjects and 455 control subjects by the iSelect Custom Infinium Genotyping system. Because 32 SNPs were dropped during the manufacturing process of custom array, we ultimately genotyped 223 SNPs. All the procedures were carried out per the manufacturer's instructions. Briefly, 150–300 ng of genomic DNA was denatured with sodium hydroxide and amplified for 20–24 h at 37 °C using the provided reagents. Samples were then fragmented for 1 h at 37 °C, precipitated by 2-propanol, and resuspended completely. After being denatured for 20 min at 95 °C, the samples were hybridized on iSelect Genotyping BeadChips (Illumina) for 16–24 h at 48 °C. Following the hybridization, the BeadChips were reacted for the single-base or allele-specific extension and stained. The BeadChips were then scanned by a BeadArray Reader (Illumina). The intensity data from each chip were loaded into BeadStudio 3.0 software (Illumina) to convert the fluorescence intensities into SNP genotyping results. To check the quality of each experiment, we analyzed the call rate (per sample) and the QC index (staining, extension, target removal, hybridization, stringency, nonspecific binding, and nonpolymorphic) using the BeadStudio software. To check gender mismatches between the clinical records and the genotyping results, we also genotyped 15 SNPs in the X chromosome. To check the quality of each data point, the SNPs were initially genotyped by clustering the 865 samples (410 case and 455 control samples) using BeadStudio (no-call threshold = 0.15). Because 6 samples showed a significantly lower call rate than the others (<95%), we reprocessed them starting with the sample preparation, as described in the manufacturer's technical note (Infinium Genotyping Data Analysis; Illumina). All the reprocessed samples showed a higher call rate than seen in the initial results. After excluding 8 samples (see *SI Results*), we performed the clustering with 857 samples (409 case and 448 control samples) for the subsequent analysis. Three independent observers (M.N., T.T., and T.Y.) visually checked the 2D cluster plots of the genotypes for all the SNPs as described, and we edited the clusters according to the manufacturer's technical note when the clusters were obviously inadequate (Fig. S3 *E* and *F*).

Logistic Regression Analysis and Calculation of Joint OR. Logistic regression analysis was performed to assess the joint contributions (with interaction) of the 6 candidate SNPs to the risk of POAG using SAS software (Version 9.1.3 on Windows; SAS Institute Japan). Because 4 SNPs (rs547984, rs540782, rs693421, and rs2499601) showed a high LD between each other, the SNP with the highest call rate (rs547984) was selected as representative of these SNPs. Consequently, we used 3 of the 6 SNPs for the analysis. For these SNPs, the case-control status and genotyping data of the samples with a call rate of 100% in stages 1 and 2 were incorporated into the analysis (743 case and 827 control samples). To model the genetic effects, we adopted an additive model and the following genetic models with classification variables: the 2-genotype model (*AA*+*AB* and *BB* or *AA* and *AB*+*BB*) and the 3-genotype model (*AA*, *AB*, and *BB*). In the 2-genotype model, either a dominant or recessive type was selected into the models by a stepwise selection method with 0.01 significance levels of entering and staying. The logistic regression models for all the possible combinations of SNPs were compared by the AIC to obtain the best-fitting model with the lowest AIC. The joint OR was calculated relative to the groups possessing the

low-risk genotype at all loci, which was defined to be a homozygote of the allele with lower frequency in cases than in controls.

Population Stratification. For stage 1, we first extracted the tag SNPs of HapMap-JPT as unrelated SNPs on the Affymetrix 500K Array Set whose values were: (*i*) ≥95% call rate per SNP in case and control samples, respectively; (*ii*) ≤5% call rate difference between case and control samples for each SNP; and (*iii*) ≥5% of MAF in case and control samples. Of the remaining 47,011 SNPs, we then selected 528 on autosomal chromosomes that were separated from each other by at least 5 Mb to be sure that they were unrelated, as reported previously (7). Using these SNPs, we ran the program for 100,000 burn-in steps, followed by 300,000 Markov Chain Monte Carlo steps from K (the assumed population number: 1–5). As a reference, we also analyzed the population stratification of samples from the HapMap Project.

For stage 2, we first extracted the tag SNPs of the HapMap-JPT from our custom array as unrelated SNPs, including the SNPs that were irrelevant to this study, whose values were (*i*) ≥95% call rate per SNP in case and control samples and (*ii*) ≥5% MAF in case and control samples. We then selected 249 SNPs on autosomal chromosomes that were separated from each other by at least 5 Mb. Using these SNPs, we ran the program under the same conditions as for stage 1.

1. Yanagiya T, et al. (2007) Association of single-nucleotide polymorphisms in MTMR9 gene with obesity. *Hum Mol Genet* 16:3017–3026.
2. Maller J, et al. (2006) Common variation in three genes, including a noncoding variant in CFH, strongly influences risk of age-related macular degeneration. *Nat Genet* 38:1055–1059.
3. Traggiai E, et al. (2004) An efficient method to make human monoclonal antibodies from memory B cells: Potent neutralization of SARS coronavirus. *Nat Med* 10:871–875.
4. European Glaucoma Society (2003) *Terminology and Guidelines for Glaucoma* (Dogma, Savona, Italy), 2nd Ed, pp 1–152.
5. Iwase A, et al. (2004) The prevalence of primary open-angle glaucoma in Japanese: The Tajimi Study. *Ophthalmology* 111:1641–1648.
6. Van Herick W, Schwartz A (1969) Estimation of width of angle of anterior chamber incidence and significance of the narrow angle. *Am J Ophthalmol* 68:626–629.
7. Sladek R, et al. (2007) A genome-wide association study identifies novel risk loci for type 2 diabetes. *Nature* 445:881–885.

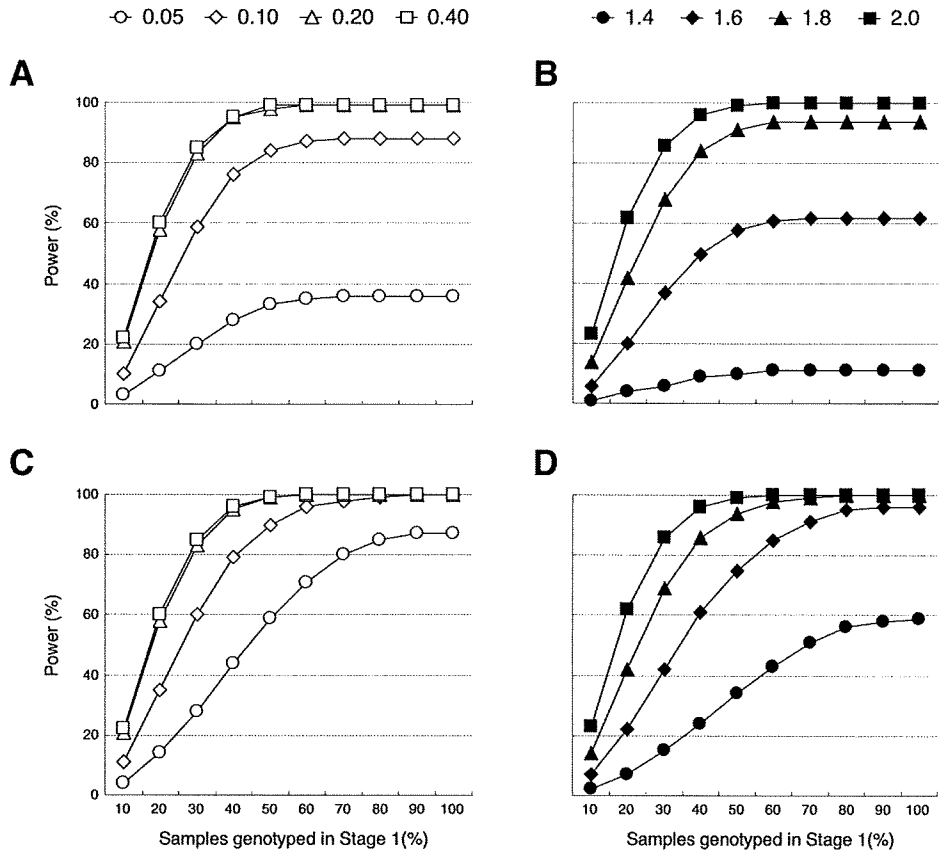

Fig. S1. Statistical power of our study calculated by CaTS software. Sample size of stage 1 plotted against the power of joint analysis (*A* and *C*) with increasing disease allele frequencies and the genotype risk ratio fixed at 2.0. (*B* and *D*) Increasing genotype risk ratios with the disease allele frequency fixed at 0.25. Significance level: 1×10^{-7} (*A* and *B*) and 1×10^{-4} (*C* and *D*).

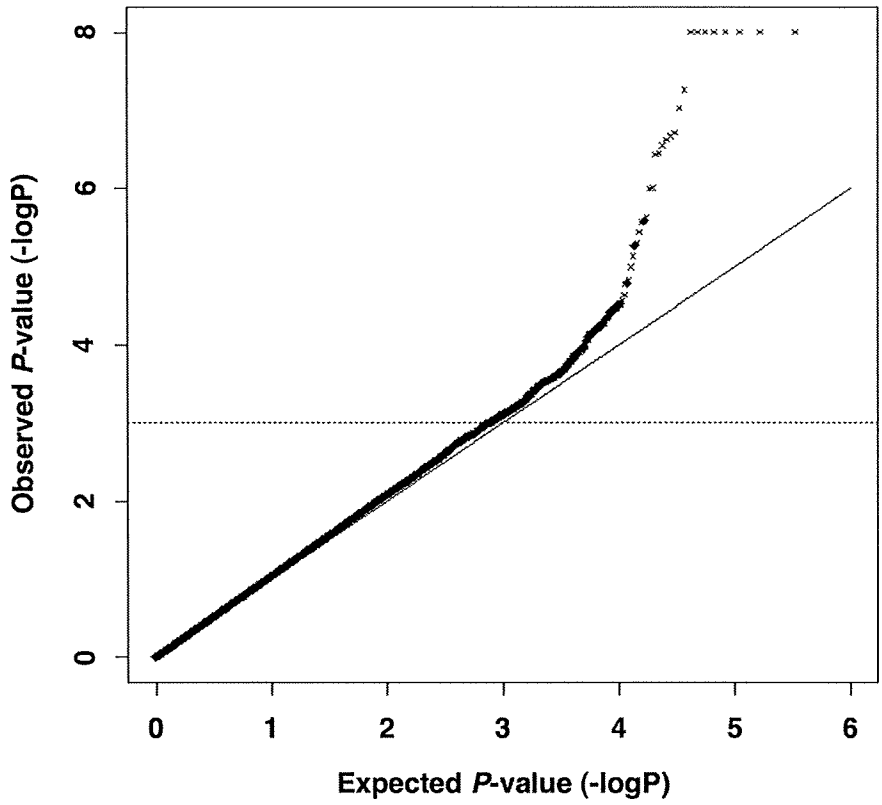

Fig. S2. Quantile-quantile plot of the 331,838 SNPs that passed our stringent QC filter in stage 1 and the SNPs selected after the visual check of 2D cluster plots (filled circles). The distribution of the expected *P* values of allele frequency comparison was plotted against the observed *P* values. Under the null hypothesis, with no disease association, the points lie on the solid line. Observed SNP *P* values smaller than 10^{-8} are plotted as 10^{-8}. The dotted line ($P = 10^{-3}$) marks the deviation of the observed *P* values from the null hypothesis.

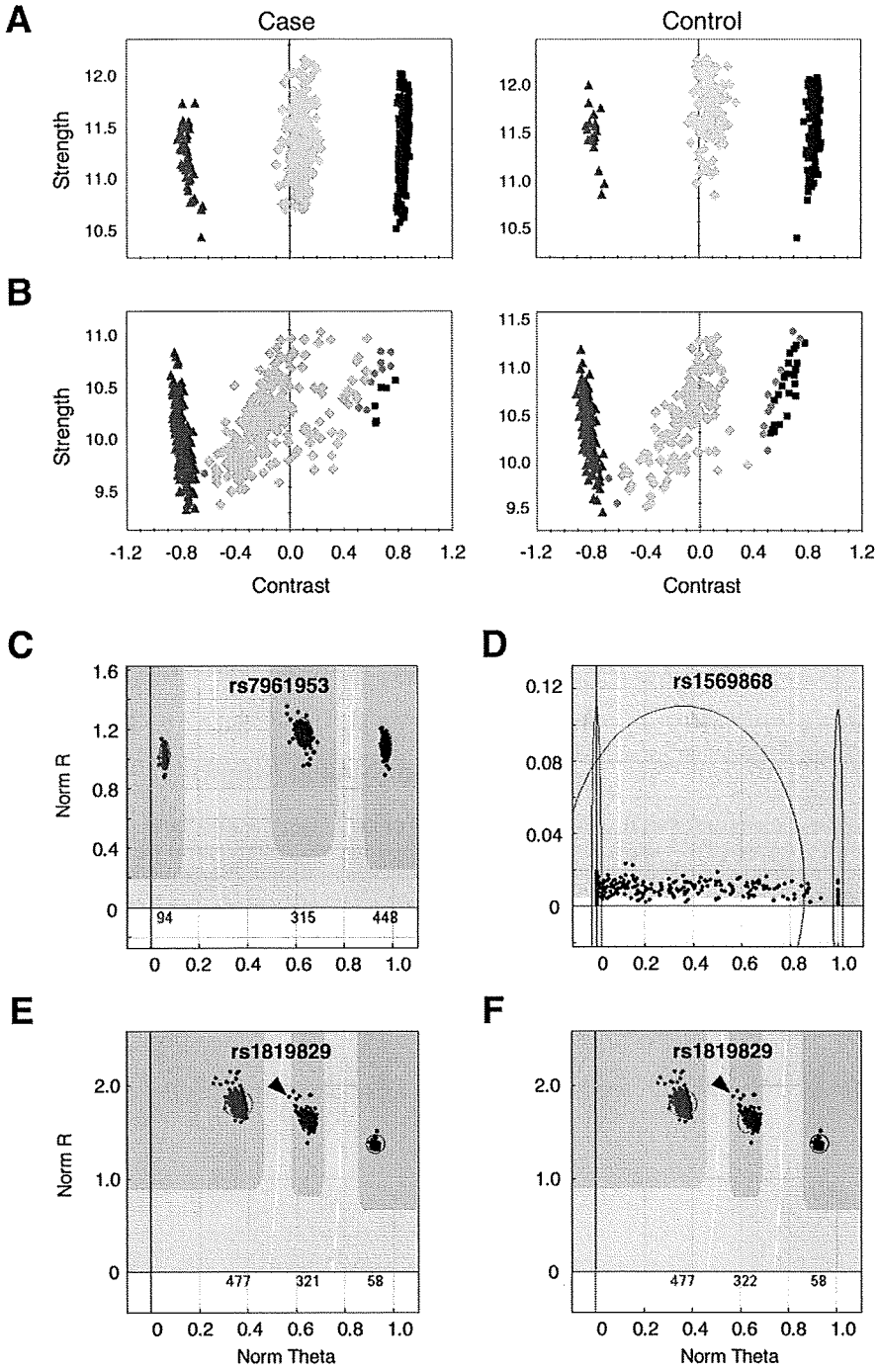

Fig. S3. Representative 2D cluster plots of the SNPs with $P < 10^{-3}$ in stage 1 and the SNPs tested in stage 2. In stage 1, 255 SNPs remained as high-confidence disease-associated SNPs after eliminating those that were not in tight clusters (see Fig. 1). (*A*) Cluster plot of rs7961953, which was given the highest possible total acceptability score (4; see *SI Materials and Methods*). (*B*) Cluster plot of rs10764881, which was given a low acceptability score of 1 (case score of 0 and control score of 1). Because the total score was less than 2 for this SNP, we eliminated it and similar poorly clustering SNPs from consideration. Homozygotic genotypes are shown in red or blue, and heterozygotic genotypes are shown in green. Genotypes that were not called are shown as gray dots. *X* axes show the allele contrast, and *Y* axes show signal strength. (*C, D, E* and *F*) We visually checked the 2D cluster plots for the 223 SNPs in stage 2 and edited some of them using BeadStudio software. (*C*) Cluster plot of rs7961953 ($P < 0.05$) showing a well-clustered SNP. (*D*) The cluster plot of rs1569868 is representative of poorly clustering SNPs that were eliminated from subsequent analysis. (*E*) Cluster plot of rs1819829 showing a point that was not called (arrowhead) and seemed to be of a heterozygous genotype. (*F*) After all the genotyping results were checked by 3 independent observers (see *SI Materials and Methods*), we judged this genotype to be heterozygous and edited the cluster to accept this SNP as shown. Homozygotic genotypes are shown in red or blue, and heterozygotic genotypes are shown in purple. Genotypes that were not called are shown as black dots. *X* axes show the normalized theta (Norm Theta), and *Y* axes show the distance from the point to the origin (Norm R).

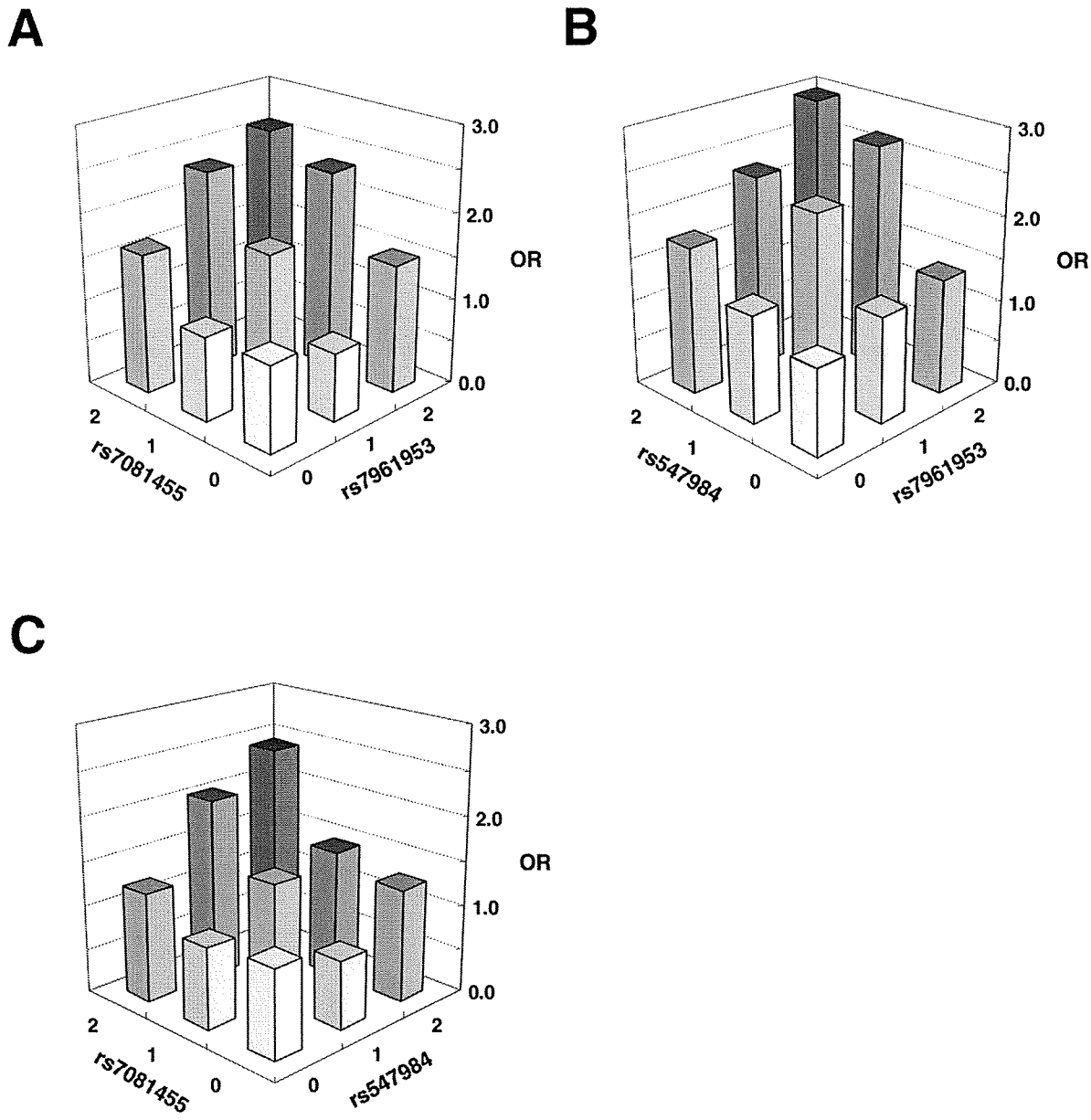

Fig. S4. Joint OR between 2 candidate SNPs. Three paired combinations among 3 candidate SNPs were calculated in a preliminary analysis. Joint ORs for the combination of rs7081455 and rs7961953 (*A*), rs547984 and rs7961953 (*B*), and rs7081455 and rs547984 (*C*) are shown. *X* and *Y* axes represent the number of risk alleles that showed higher frequency in case samples than in control samples. *Z* axis represents the joint OR relative to the group possessing the lower risk genotype of the 2 SNPs.

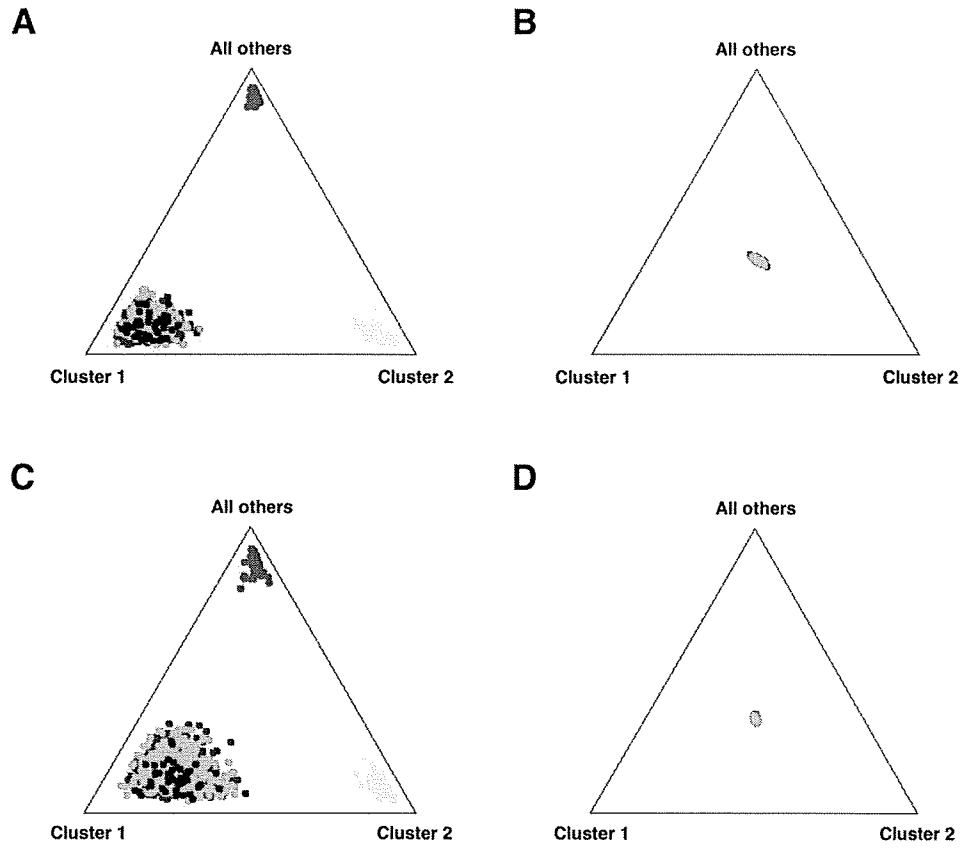

Fig. S5. Population stratification analysis of sample data for all the subjects participating in this study, analyzed by STRUCTURE software. Data are shown in triangle plots (*K*, assumed number of populations; $K = 3$). The analysis shows the populations used in stages 1 (*A*) and 2 (*C*) (case and control groups) and the HapMap-JPT separated from the HapMap-CEU and -YRI with a highest log likelihood of $K = 3$. When the analysis was restricted to the DNA samples used in stages 1 (*B*) and 2 (*D*), plots showed a single tight cluster with a highest log likelihood of $K = 1$. Red and green dots correspond to case and control samples, respectively. Blue, yellow, and pink dots correspond to the HapMap-JPT, -CEU, and -YRI samples, respectively.

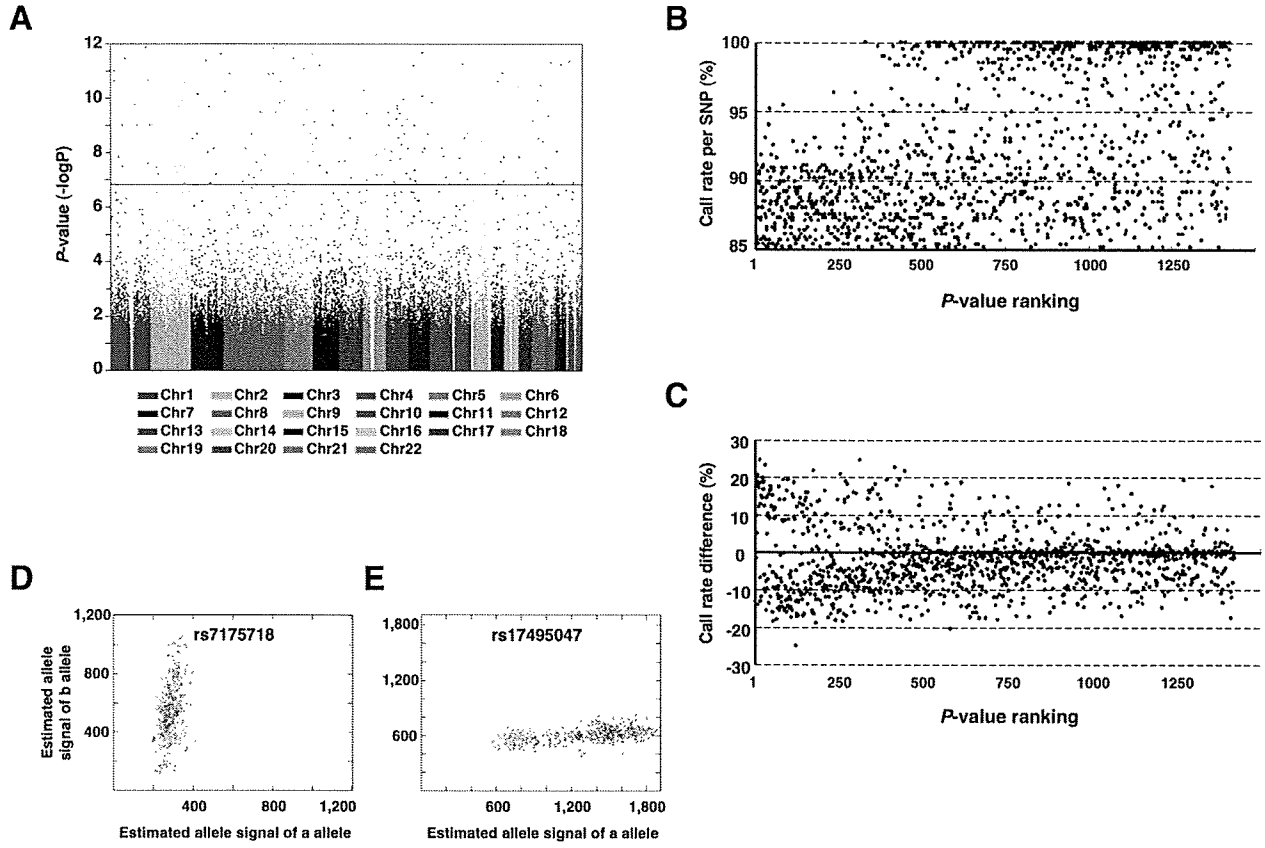

Fig. S6. Low-quality SNPs showed a high association with disease using the standard filter. In our preliminary experiments, we used the standard filter (≥85% call rate per SNP and ≥5% MAF in case and control data) to determine the *P* value for allele frequency comparison. The results were plotted in the order of chromosomes, using the R software. (*A*) Horizontal line, threshold for Bonferroni's correction. Call rate for high-ranked SNPs (*B*) and the difference in call rate between case and control samples (*C*), plotted in order of *P* value. (*D, E*) Examples of 2D cluster plots of case plus control results for low-quality SNPs. (*D*) For rs7175718, the *P* value for allele frequency comparison, call rate, and call rate difference were $P = 1.4 \times 10^{-17}$, 89%, and 18.3%, respectively. (*E*) For rs17495047, the *P* value for allele frequency comparison, call rate, and call rate difference were 7.7×10^{-15}, 88%, and 9.8%, respectively. Homozygotic genotypes for the different alleles are shown in purple or blue, and heterozygotic genotypes are shown in green. Genotypes that were not called are shown as red dots.